Designing complementary filters for sensor fusion using $\mathcal{H}_\infty$ synthesis

Thomas Dehaeze[a,b,*], Mohit Verma[c,d], Christophe Collette[b,d]

[a]*European Synchrotron Radiation Facility, Grenoble, France*

[b]*University of Liège, PML, Department of Aerospace and Mechanical Engineering, 4000 Liège, Belgium.*

[c]*CSIR — Structural Engineering Research Centre, Taramani, Chennai — 600113, India.*

[d]*Université Libre de Bruxelles, Precision Mechatronics Laboratory, BEAMS Department, 1050 Brussels, Belgium.*

Abstract

In order to obtain a better estimate of a quantity being measured, several sensors having different characteristics can be merged with a technique called "sensor fusion". The obtained "super sensor" can combine the benefits of the individual sensors provided that the complementary filters used in the fusion are well designed. Indeed, properties of the super sensor are linked to the magnitude of the complementary filters. Properly shaping the magnitude of complementary filters is a difficult and time-consuming task. In this study, we address this issue and propose a new method for designing complementary filters. This method uses weighting functions to specify the wanted shape of the complementary filter that are then easily obtained using the standard $\mathcal{H}_\infty$ synthesis. The proper choice of the weighting functions is discussed, and the effectiveness and simplicity of the design method is highlighted using several examples. Such synthesis method is further extended for the shaping of more than two complementary filters.

Keywords: Sensor fusion, Complementary filters, $\mathcal{H}_\infty$ synthesis, Vibration isolation, Motion control

1. Introduction

Measuring a physical quantity using sensors is always subject to several limitations. First, the accuracy of the measurement will be affected by several noise sources, such as electrical noise of the conditioning electronics being used. Second, the frequency range in which the measurement is relevant is bounded by the bandwidth of the sensor. One way to overcome these limitations is to combine several sensors using a technique called "sensor fusion" [1]. Fortunately, a wide variety of sensors exist, each with different characteristics. By carefully choosing the fused sensors, a so called "super sensor" is obtained that combines benefits of individual sensors.

In some situations, sensor fusion is used to increase the bandwidth of the measurement [2–4]. For instance, in [2], the bandwidth of a position sensor is increased by fusing it with an accelerometer providing the high frequency motion information. For other applications, sensor fusion is used to obtain an estimate of the measured quantity with lower noise [5–8]. More recently, the fusion of sensors measuring different physical quantities has been proposed to obtain interesting properties for control [9, 10]. In [9], an inertial sensor used for active vibration isolation is fused with a sensor collocated with the actuator for improving the stability margins of the feedback controller.

Practical applications of sensor fusion are numerous. It is widely used for the attitude estimation of several autonomous vehicles such as unmanned aerial vehicle [11–13] and underwater vehicles [14, 15]. Naturally, it is of great benefits for high performance positioning control as shown in [2–4, 10]. Sensor fusion was also shown to be a key technology to improve the performance of active vibration isolation systems [16]. Emblematic examples are the isolation stages of gravitational wave detectors [9, 17] such as the ones used at the LIGO [5, 6] and at the VIRGO [18].

---

[*]Corresponding author. Email Address: thomas.dehaeze@esrf.fr

There are mainly two ways to perform sensor fusion: either using a set of complementary filters [19] or using Kalman filtering [20, 21]. For sensor fusion applications, both methods are sharing many relationships [8, 20, 22, 23]. However, for Kalman filtering, we are forced to make assumption about the probabilistic character of the sensor noises [8] whereas it is not the case with complementary filters. Furthermore, the advantages of complementary filters over Kalman filtering for sensor fusion are their general applicability, their low computational cost [22], and the fact that they are intuitive as their effects can be easily interpreted in the frequency domain.

A set of filters is said to be complementary if the sum of their transfer functions is equal to one at all frequencies. In the early days of complementary filtering, analog circuits were employed to physically realize the filters [19]. Analog complementary filters are still used today [10, 24], but most of the time they are now implemented digitally as it allows for much more flexibility.

Several design methods have been developed over the years to optimize complementary filters. The easiest way to design complementary filters is to use analytical formulas. Depending on the application, the formulas used are of first order [10, 12, 25], second order [11, 13, 26] or even higher orders [2, 3, 9, 26, 27].

As the characteristics of the "super sensor" depends on the design of the complementary filters [28], several optimization techniques have been developed over the years. Some are based on the finding optimal parameters of analytical formulas [4, 13, 23], while other are using convex optimization tools [5, 6] such as linear matrix inequalities [14]. As shown in [7], the design of complementary filters can also be linked to the standard mixed-sensitivity control problem. Therefore, all the powerful tools developed for the classical control theory can also be used for the design of complementary filters. For instance, in [13] the two gains of a Proportional Integral (PI) controller are optimized to minimize the noise of the super sensor.

The common objective of all these complementary filters design methods is to obtain a super sensor that has desired characteristics, usually in terms of noise and dynamics. Moreover, as reported in [3, 7], phase shifts and magnitude bumps of the "super sensors" dynamics can be observed if either the complementary filters are poorly designed or if the sensors are not well calibrated. Therefore, the robustness of the fusion is also of concerned when designing the complementary filters. Although many design methods of complementary filters have been proposed in the literature, no simple method that allows to specify the desired super sensor characteristic while ensuring good fusion robustness has been proposed.

Fortunately, both the robustness of the fusion and the super sensor characteristics can be linked to the magnitude of the complementary filters [28]. Based on that, this paper introduces a new way to design complementary filters using the $\mathcal{H}_\infty$ synthesis which allows to shape the magnitude of the complementary filters in an easy and intuitive way.

Section 2 introduces the sensor fusion architecture and demonstrates how typical requirements can be linked to the complementary filters magnitudes. In Section 3, the shaping of complementary filters is formulated as an $\mathcal{H}_\infty$ optimization problem using weighting functions, and the simplicity of the proposed method is illustrated with an example. The synthesis method is further validated in Section 4 by designing complex complementary filters. Section 5 compares the proposed synthesis method with the classical mixed-sensitivity synthesis, and extends it to the shaping of more than two complementary filters.

2. Sensor Fusion and Complementary Filters Requirements

Complementary filters provides a framework for fusing signals from different sensors. As the effectiveness of the fusion depends on the proper design of the complementary filters, they are expected to fulfill certain requirements. These requirements are discussed in this section.

2.1. Sensor Fusion Architecture

A general sensor fusion architecture using complementary filters is shown in Fig. 1 where several sensors (here two) are measuring the same physical quantity x. The two sensors output signals $\hat{x}_1$ and $\hat{x}_2$ are estimates of x. Each of these estimates are then filtered out by complementary filters and combined to form a new estimate $\hat{x}$.

The resulting sensor, termed as super sensor, can have larger bandwidth and better noise characteristics in comparison to the individual sensor. This means that the super sensor provides an estimate $\hat{x}$ of x which can be more accurate over a larger frequency band than the outputs of the individual sensors.
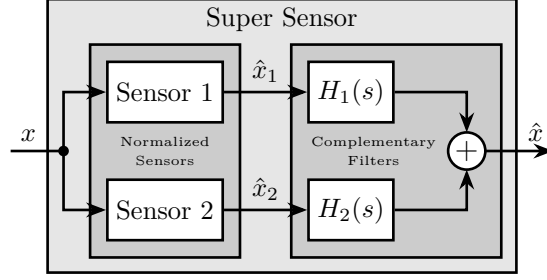

Figure 1: Schematic of a sensor fusion architecture using complementary filters.

The complementary property of filters $H_1(s)$ and $H_2(s)$ implies that the sum of their transfer functions is equal to unity. That is, unity magnitude and zero phase at all frequencies. Therefore, a pair of complementary filter needs to satisfy the following condition:

$$H_1(s) + H_2(s) = 1 \tag{1}$$

It will soon become clear why the complementary property is important for the sensor fusion architecture.

2.2. Sensor Models and Sensor Normalization

In order to study such sensor fusion architecture, a model for the sensors is required. Such model is shown in Fig. 2a and consists of a linear time invariant (LTI) system $G_i(s)$ representing the sensor dynamics and an input n_i representing the sensor noise. The model input x is the measured physical quantity and its output $\tilde{x}_i$ is the "raw" output of the sensor.

Before filtering the sensor outputs $\tilde{x}_i$ by the complementary filters, the sensors are usually normalized to simplify the fusion. This normalization consists of using an estimate $\hat{G}_i(s)$ of the sensor dynamics $G_i(s)$, and filtering the sensor output by the inverse of this estimate $\hat{G}_i^{-1}(s)$ as shown in Fig. 2b. It is here supposed that the sensor inverse $\hat{G}_i^{-1}(s)$ is proper and stable. This way, the units of the estimates $\hat{x}_i$ are equal to the units of the physical quantity x. The sensor dynamics estimate $\hat{G}_1(s)$ can be a simple gain or a more complex transfer function.
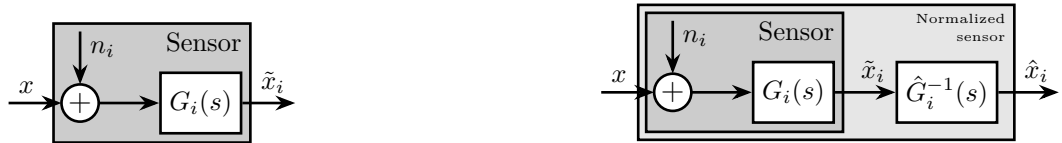
(a) Basic sensor model consisting of a noise input n_i and a linear time invariant transfer function $G_i(s)$.

(b) Normalized sensors using the inverse of an estimate $\hat{G}_i(s)$ of the sensor dynamics.

Figure 2: Sensor models with and without normalization.

Two normalized sensors are then combined to form a super sensor as shown in Fig. 3. The two sensors are measuring the same physical quantity x with dynamics $G_1(s)$ and $G_2(s)$, and with *uncorrelated* noises n_1 and n_2. The signals from both normalized sensors are fed into two complementary filters $H_1(s)$ and $H_2(s)$ and then combined to yield an estimate $\hat{x}$ of x.

The super sensor output is therefore equal to:

$$\hat{x} = \left(H_1(s)\hat{G}_1^{-1}(s)G_1(s) + H_2(s)\hat{G}_2^{-1}(s)G_2(s)\right)x + H_1(s)\hat{G}_1^{-1}(s)G_1(s)n_1 + H_2(s)\hat{G}_2^{-1}(s)G_2(s)n_2 \tag{2}$$
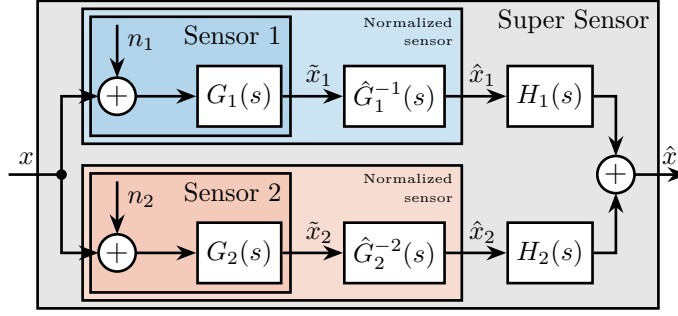
Figure 3: Sensor fusion architecture with two normalized sensors.

2.3. Noise Sensor Filtering

In this section, it is supposed that all the sensors are perfectly normalized, such that:

$$\frac{\hat{x}_i}{x} = \hat{G}_i(s)G_i(s) = 1 \tag{3}$$

The effect of a non-perfect normalization will be discussed in the next section.

Provided (3) is verified, the super sensor output $\hat{x}$ is then:

$$\hat{x} = x + H_1(s)n_1 + H_2(s)n_2 \tag{4}$$

From (4), the complementary filters $H_1(s)$ and $H_2(s)$ are shown to only operate on the sensor's noises. Thus, this sensor fusion architecture permits to filter the noise of both sensors without introducing any distortion in the physical quantity to be measured. This is why the two filters must be complementary.

The estimation error δx, defined as the difference between the sensor output $\hat{x}$ and the measured quantity x, is computed for the super sensor (5).

$$\delta x \triangleq \hat{x} - x = H_1(s)n_1 + H_2(s)n_2 \tag{5}$$

As shown in (6), the Power Spectral Density (PSD) of the estimation error $\Phi_{\delta x}$ depends both on the norm of the two complementary filters and on the PSD of the noise sources Φ_{n_1} and Φ_{n_2}.

$$\Phi_{\delta x}(\omega) = |H_1(j\omega)|^2 \Phi_{n_1}(\omega) + |H_2(j\omega)|^2 \Phi_{n_2}(\omega) \tag{6}$$

If the two sensors have identical noise characteristics, $\Phi_{n_1}(\omega) = \Phi_{n_2}(\omega)$, a simple averaging ($H_1(s) = H_2(s) = 0.5$) is what would minimize the super sensor noise. This is the simplest form of sensor fusion with complementary filters.

However, the two sensors have usually high noise levels over distinct frequency regions. In such case, to lower the noise of the super sensor, the norm $|H_1(j\omega)|$ has to be small when $\Phi_{n_1}(\omega)$ is larger than $\Phi_{n_2}(\omega)$ and the norm $|H_2(j\omega)|$ has to be small when $\Phi_{n_2}(\omega)$ is larger than $\Phi_{n_1}(\omega)$. Therefore, by properly shaping the norm of the complementary filters, it is possible to minimize the noise of the super sensor noise.

2.4. Sensor Fusion Robustness

In practical systems the sensor normalization is not perfect and condition (3) is not verified.

In order to study such imperfection, a multiplicative input uncertainty is added to the sensor dynamics (Fig. 4a). The nominal model is taken as the estimated model for the normalization $\hat{G}_i(s)$, Δ_i is any stable transfer function satisfying $|\Delta_i(j\omega)| \leq 1$, $\forall \omega$, and $w_i(s)$ is a weighting transfer function representing the magnitude of the uncertainty.

The weight $w_i(s)$ is chosen such that the real sensor dynamics $G(j\omega)$ is contained in the uncertain region represented by a circle in the complex plane, centered on 1 and with a radius equal to $|w_i(j\omega)|$.

As the nominal sensor dynamics is taken as the normalized filter, the normalized sensor can be further simplified as shown in Fig. 4b.
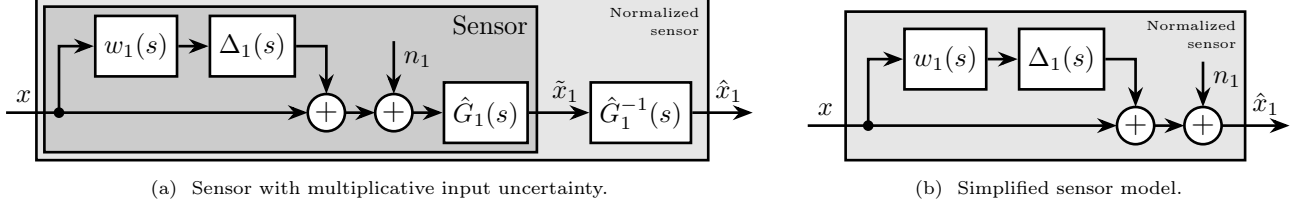

(a) Sensor with multiplicative input uncertainty.

(b) Simplified sensor model.

Figure 4: Sensor models with dynamical uncertainty.

The sensor fusion architecture with two sensor models including dynamical uncertainty is shown in Fig. 5.
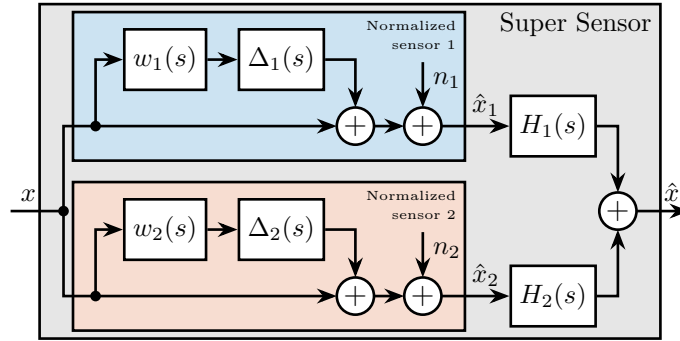

Figure 5: Sensor fusion architecture with sensor dynamics uncertainty.

The super sensor dynamics (7) is no longer equal to 1 and now depends on the sensor dynamical uncertainty weights $w_i(s)$ as well as on the complementary filters $H_i(s)$.

$$\frac{\hat{x}}{x} = 1 + w_1(s)H_1(s)\Delta_1(s) + w_2(s)H_2(s)\Delta_2(s) \tag{7}$$

The dynamical uncertainty of the super sensor can be graphically represented in the complex plane by a circle centered on 1 with a radius equal to $|w_1(j\omega)H_1(j\omega)| + |w_2(j\omega)H_2(j\omega)|$ as shown in Fig. 6.
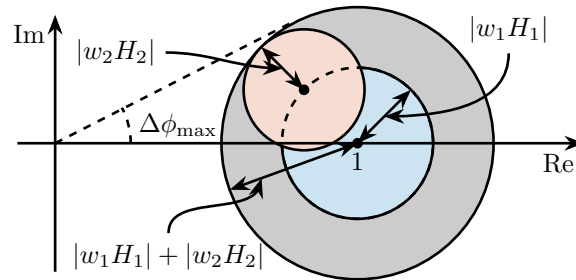

Figure 6: Uncertainty region of the super sensor dynamics in the complex plane (grey circle). The contribution of both sensors 1 and 2 to the total uncertainty are represented respectively by a blue circle and a red circle. The frequency dependency ω is here omitted.

The super sensor dynamical uncertainty, and hence the robustness of the fusion, clearly depends on the complementary filters norms. For instance, the phase $\Delta\phi(\omega)$ added by the super sensor dynamics at frequency ω is bounded by $\Delta\phi_{\max}(\omega)$ which can be found by drawing a tangent from the origin to the uncertainty circle of the super sensor (Fig. 6). Therefore, the phase uncertainty of the super sensor dynamics depends on the Complementary filters norms (8).

$$\Delta\phi_{\max}(\omega) = \arcsin\left(|w_1(j\omega)H_1(j\omega)| + |w_2(j\omega)H_2(j\omega)|\right) \tag{8}$$

As it is generally desired to limit the maximum phase added by the super sensor, $H_1(s)$ and $H_2(s)$ should be designed such that $\Delta\phi$ is bounded to acceptable values. Typically, the norm of the complementary filter $|H_i(j\omega)|$ should be made small when $|w_i(j\omega)|$ is large, i.e., at frequencies where the sensor dynamics is uncertain.

3. Complementary Filters Shaping

As shown in Section 2, the noise and robustness of the super sensor are a function of the complementary filters norms. Therefore, a complementary filters synthesis method that allows to shape their norms would be of great use. In this section, such synthesis is proposed by writing the synthesis objective as a standard $\mathcal{H}_\infty$ optimization problem. As weighting functions are used to represent the wanted complementary filters shapes during the synthesis, the proper design of weighting functions is discussed. Finally, the synthesis method is validated on an simple example.

3.1. Synthesis Objective

The synthesis objective is to shape the norm of two filters $H_1(s)$ and $H_2(s)$ while ensuring their complementary property (1). This is equivalent as to finding proper and stable transfer functions $H_1(s)$ and $H_2(s)$ such that conditions (9a), (9b) and (9c) are satisfied.

$$H_1(s) + H_2(s) = 1 \tag{9a}$$

$$|H_1(j\omega)| \leq \frac{1}{|W_1(j\omega)|} \quad \forall\omega \tag{9b}$$

$$|H_2(j\omega)| \leq \frac{1}{|W_2(j\omega)|} \quad \forall\omega \tag{9c}$$

$W_1(s)$ and $W_2(s)$ are two weighting transfer functions that are carefully chosen to specify the maximum wanted norms of the complementary filters during the synthesis.

3.2. Shaping of Complementary Filters using $\mathcal{H}_\infty$ synthesis

In this section, it is shown that the synthesis objective can be easily expressed as a standard $\mathcal{H}_\infty$ optimization problem and therefore solved using convenient tools readily available.

Consider the generalized plant $P(s)$ shown in Fig. 7a and mathematically described by (10).

$$\begin{bmatrix} z_1 \\ z_2 \\ v \end{bmatrix} = P(s)\begin{bmatrix} w \\ u \end{bmatrix}; \quad P(s) = \begin{bmatrix} W_1(s) & -W_1(s) \\ 0 & W_2(s) \\ 1 & 0 \end{bmatrix} \tag{10}$$

Applying the standard $\mathcal{H}_\infty$ synthesis on the generalized plant $P(s)$ is then equivalent as finding a stable filter $H_2(s)$ which based on v, generates a signal u such that the $\mathcal{H}_\infty$ norm of the system in Fig. 7b from w to $[z_1, \ z_2]$ is less than one (11).

$$\left\| \begin{matrix} (1 - H_2(s)) \, W_1(s) \\ H_2(s)W_2(s) \end{matrix} \right\|_\infty \leq 1 \tag{11}$$

By then defining $H_1(s)$ to be the complementary of $H_2(s)$ (12), the $\mathcal{H}_\infty$ synthesis objective becomes equivalent to (13) which ensure that (9b) and (9c) are satisfied.
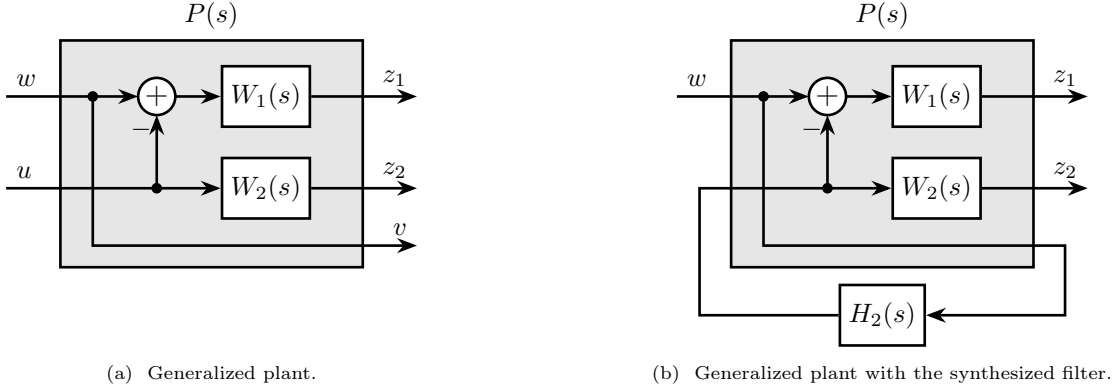
6

(a) Generalized plant.

(b) Generalized plant with the synthesized filter.

Figure 7: Architecture for the $\mathcal{H}_\infty$ synthesis of complementary filters.

$$H_1(s) \triangleq 1 - H_2(s) \tag{12}$$

$$\left\| \begin{matrix} H_1(s)W_1(s) \\ H_2(s)W_2(s) \end{matrix} \right\|_\infty \leq 1 \tag{13}$$

Therefore, applying the $\mathcal{H}_\infty$ synthesis on the standard plant $P(s)$ (10) will generate two filters $H_2(s)$ and $H_1(s) \triangleq 1 - H_2(s)$ that are complementary (9) and such that there norms are bellow specified bounds (9b), (9c).

Note that there is not an equivalence between the $\mathcal{H}_\infty$ norm condition (13) and the initial synthesis objectives (9b) and (9c), but only an implication. Hence, the optimization may be a little bit conservative with respect to the "set" of filters on which it is performed. There might be solutions were the objectives (9b) and (9c) are valid but where the $\mathcal{H}_\infty$ norm (13) is larger than one. In practice, this is however not an found to be an issue.

3.3. Weighting Functions Design

Weighting functions are used during the synthesis to specify the maximum allowed norms of the complementary filters. The proper design of these weighting functions is of primary importance for the success of the presented $\mathcal{H}_\infty$ synthesis of complementary filters.

First, only proper and stable transfer functions should be used. Second, the order of the weighting functions should stay reasonably small in order to reduce the computational costs associated with the solving of the optimization problem and for the physical implementation of the filters (the order of the synthesized filters being equal to the sum of the weighting functions orders). Third, one should not forget the fundamental limitations imposed by the complementary property (1). This implies for instance that $|H_1(j\omega)|$ and $|H_2(j\omega)|$ cannot be made small at the same frequency.

When designing complementary filters, it is usually desired to specify their slopes, their "blending" frequency and their maximum gains at low and high frequency. To help with the design of the weighting functions such that the above specification can be easily expressed, the formula (14) is proposed.

$$W(s) = \left(\frac{\frac{1}{\omega_c} \sqrt{\frac{1 - \left(\frac{G_0}{G_c}\right)^{\frac{2}{n}}}{1 - \left(\frac{G_c}{G_\infty}\right)^{\frac{2}{n}}}} s + \left(\frac{G_0}{G_c}\right)^{\frac{1}{n}}}{\left(\frac{1}{G_\infty}\right)^{\frac{1}{n}} \frac{1}{\omega_c} \sqrt{\frac{1 - \left(\frac{G_0}{G_c}\right)^{\frac{2}{n}}}{1 - \left(\frac{G_c}{G_\infty}\right)^{\frac{2}{n}}}} s + \left(\frac{1}{G_c}\right)^{\frac{1}{n}}} \right)^n \tag{14}$$

The parameters in formula (14) are:

- $G_0 = \lim_{\omega \to 0} |W(j\omega)|$: the low frequency gain

- $G_\infty = \lim_{\omega \to \infty} |W(j\omega)|$: the high frequency gain

- $G_c = |W(j\omega_c)|$: the gain at a specific frequency ω_c in rad/s.

- n: the slope between high and low frequency. It also corresponds to the order of the weighting function.

The parameters G_0, G_c and G_∞ should either satisfy condition (15a) or (15b).

$$G_0 < 1 < G_\infty \text{ and } G_0 < G_c < G_\infty \tag{15a}$$
$$G_\infty < 1 < G_0 \text{ and } G_\infty < G_c < G_0 \tag{15b}$$

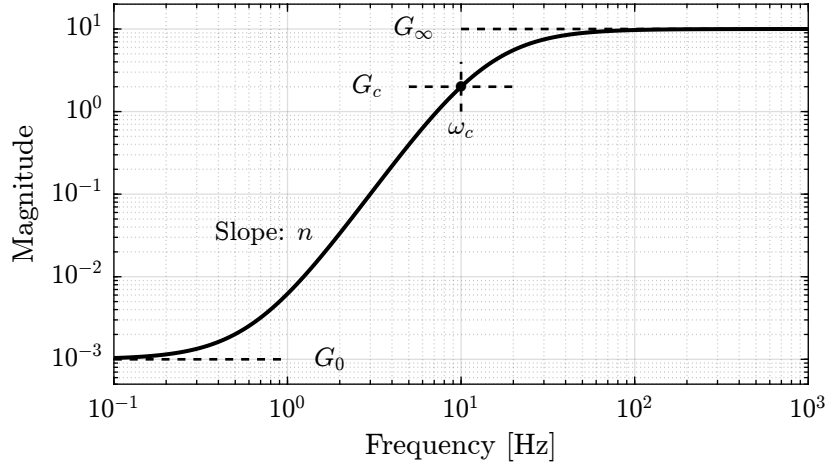An example of the obtained magnitude of a weighting function generated using (14) is shown in Fig. 8.

Figure 8: Magnitude of a weighting function generated using the proposed formula (14), $G_0 = 1e^{-3}$, $G_\infty = 10$, $\omega_c = 10\,\text{Hz}$, $G_c = 2$, $n = 3$.

3.4. Validation of the proposed synthesis method

The proposed methodology for the design of complementary filters is now applied on a simple example where two complementary filters $H_1(s)$ and $H_2(s)$ have to be designed such that:

- the blending frequency is around $10\,\text{Hz}$

- the slope of $|H_1(j\omega)|$ is $+2$ below $10\,\text{Hz}$, its low frequency gain is 10^{-3}

- the slope of $|H_2(j\omega)|$ is -3 above $10\,\text{Hz}$, its high frequency gain is 10^{-3}

The first step is to translate the above requirements into the design of the weighting functions. The proposed formula (14) is here used for such purpose. Parameters used are summarized in Table 1. The inverse magnitudes of the designed weighting functions, which are representing the maximum allowed norms of the complementary filters, are shown by the dashed lines in Fig. 9.

The $\mathcal{H}_\infty$ synthesis is then applied to the generalized plant of Fig. 7a on efficiently solved in Matlab [29] using the Robust Control Toolbox. The filter $H_2(s)$ that minimizes the $\mathcal{H}_\infty$ norm between w and $[z_1,\ z_2]^T$ is obtained. The $\mathcal{H}_\infty$ norm is here found to be close to one (16) which indicates that the synthesis is successful: the complementary filters norms are below the maximum specified upper bounds. This is confirmed by the bode plots of the obtained complementary filters in Fig. 10.

Parameters	$W_1(s)$	$W_2(s)$
G_0	0.1	1000
G_∞	1000	0.1
ω_c	$2\pi \cdot 10$	$2\pi \cdot 10$
G_c	0.45	0.45
n	2	3

Table 1: Parameters used for weighting functions $W_1(s)$ and $W_2(s)$ using (14).
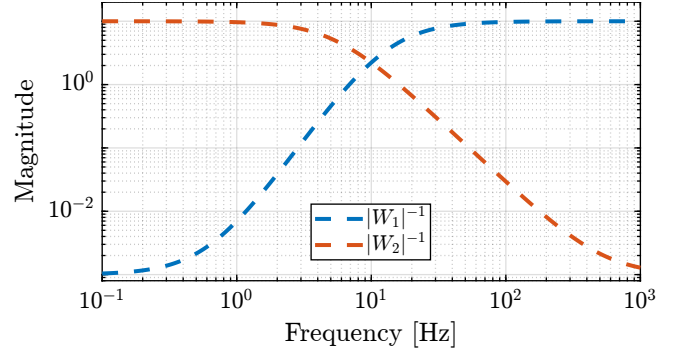
Figure 9: Inverse magnitude of the weighting functions.

$$\left\| \begin{matrix} (1 - H_2(s)) W_1(s) \\ H_2(s) W_2(s) \end{matrix} \right\|_\infty \approx 1 \tag{16}$$

Their transfer functions in the Laplace domain are given in (17). As expected, the obtained filters are of order 5, that is the sum of the weighting functions orders.

$$H_2(s) = \frac{(s + 6.6e^4)(s + 160)(s + 4)^3}{(s + 6.6e^4)(s^2 + 106s + 3e^3)(s^2 + 72s + 3580)} \tag{17a}$$

$$H_1(s) \triangleq H_2(s) - 1 = \frac{10^{-8}(s + 6.6e^9)(s + 3450)^2(s^2 + 49s + 895)}{(s + 6.6e^4)(s^2 + 106s + 3e^3)(s^2 + 72s + 3580)} \tag{17b}$$
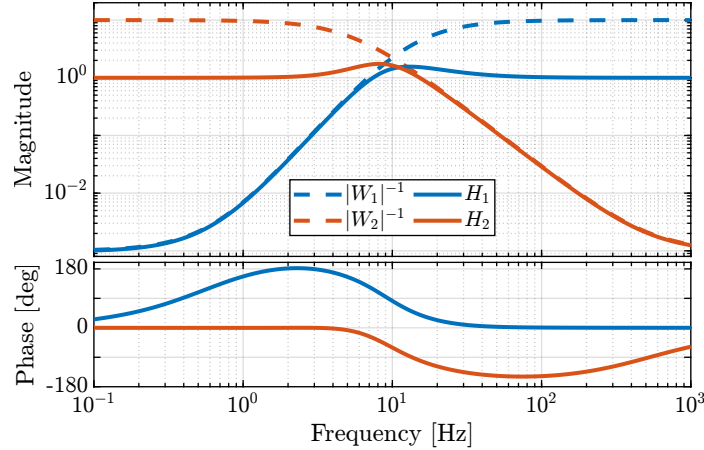

Figure 10: Bode plot of the obtained complementary filters.

This simple example illustrates the fact that the proposed methodology for complementary filters shaping is easy to use and effective. A more complex real life example is taken up in the next section.

4. Application: Design of Complementary Filters used in the Active Vibration Isolation System at the LIGO

Sensor fusion using complementary filters are widely used in active vibration isolation systems in gravitational wave detectors such at the LIGO [5, 27], the VIRGO [17, 18] and the KAGRA [30, Chap. 5].

In the first isolation stage at the LIGO, two sets of complementary filters are used and included in a feedback loop [31]. A set of complementary filters (L_2, H_2) is first used to fuse a seismometer and a geophone. Then, another set of complementary filters (L_1, H_1) is used to merge the output of the first "inertial super sensor" with a position sensor. A simplified block diagram of the sensor fusion architecture is shown in Fig. 11.
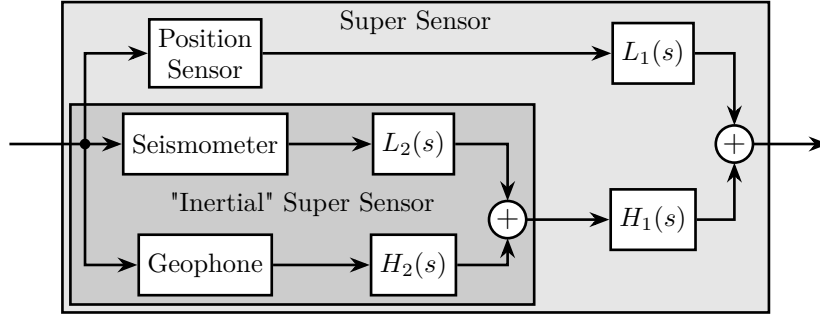

Figure 11: Simplified block diagram of the sensor blending strategy for the first stage at the LIGO [31].

The fusion of the position sensor at low frequency with the "inertial super sensor" at high frequency using the complementary filters (L_1, H_1) is done for several reasons, first of which is to give the super sensor a DC sensibility and therefore allow the feedback loop to have authority at zero frequency. The requirements on those filters are stringent and thus their design is complex and should be expressed as an optimization problem.

The approach used in [5] is to use FIR complementary filters and to write the synthesis as a convex optimization problem. After synthesis, the obtained FIR filters were found to be compliant with the requirements. However they are of high order so their implementation is quite complex. In this section, the effectiveness of the proposed complementary filter synthesis strategy is demonstrated on the same set of requirements.

4.1. Complementary Filters Specifications

The specifications for the set of complementary filters (L_1, H_1) used at the LIGO are summarized below (for further details, refer to [6]):

- From 0 to 0.008 Hz, the magnitude $|L_1(j\omega)|$ should be less or equal to 8×10^{-4}
- Between 0.008 Hz to 0.04 Hz, the filter $L_1(s)$ should attenuate the input signal proportional to frequency cubed
- Between 0.04 Hz to 0.1 Hz, the magnitude $|L_1(j\omega)|$ should be less than 3
- Above 0.1 Hz, the magnitude $|H_1(j\omega)|$ should be less than 0.045

These specifications are therefore upper bounds on the complementary filters' magnitudes. They are physically represented in Fig. 12 as well as the obtained magnitude of the FIR filters in [5].

4.2. Weighting Functions Design

The weighting functions should be designed such that their inverse magnitude is as close as possible to the specifications in order to not over-constrain the synthesis problem. However, the order of each weight should stay reasonably small in order to reduce the computational costs of the optimization problem as well as for the physical implementation of the filters.

A Type I Chebyshev filter of order 20 is used for the weighting transfer function $W_L(s)$ corresponding to the low pass filter. For the one corresponding to the high pass filter $W_H(s)$, a 7th order transfer function is designed. The magnitudes of the weighting functions are shown in Fig. 13.
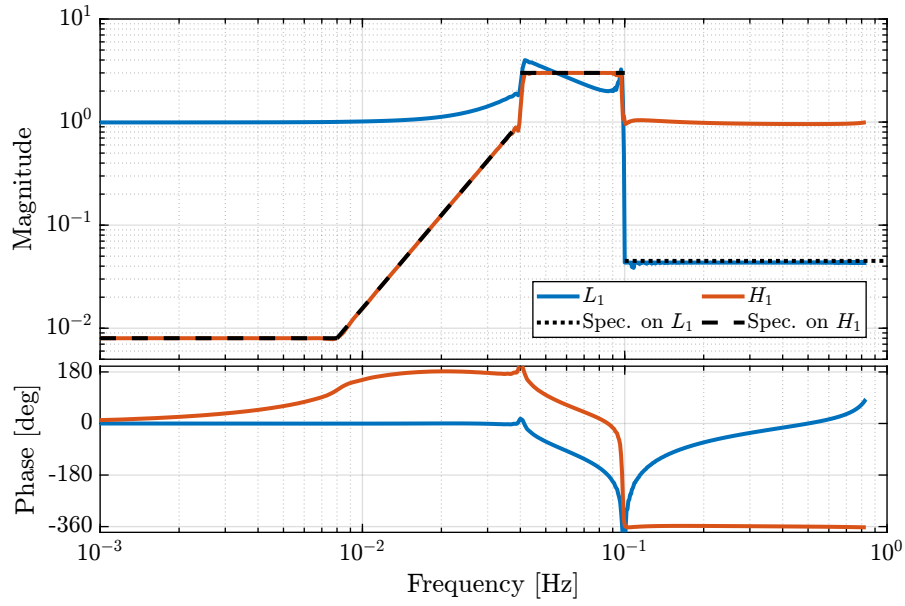
Figure 12: Specifications and Bode plot of the obtained FIR complementary filters in [5]. The filters are here obtained using the SeDuMi Matlab toolbox [32].
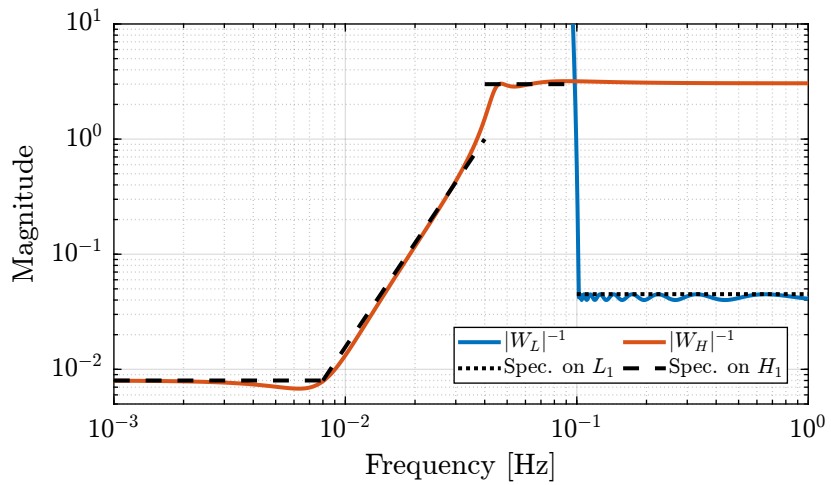

Figure 13: Specifications and weighting functions inverse magnitudes.

4.3. $\mathcal{H}_\infty$ Synthesis of the complementary filters

The proposed $\mathcal{H}_\infty$ synthesis is performed on the generalized plant shown in Fig. 7a. After optimization, the $\mathcal{H}_\infty$ norm from w to $[z_1, \ z_2]^T$ is found close to one indication successful synthesis. In Fig. 14, the bode plot of the obtained complementary filters are compared with the FIR filters of order 512 obtained in [5]. Even though the complementary filters using the $\mathcal{H}_\infty$ synthesis are of much lower order (order 27), they are found to be close to the FIR filters. This confirms the effectiveness of the proposed synthesis method even when the complementary filters are subject to complex requirements.
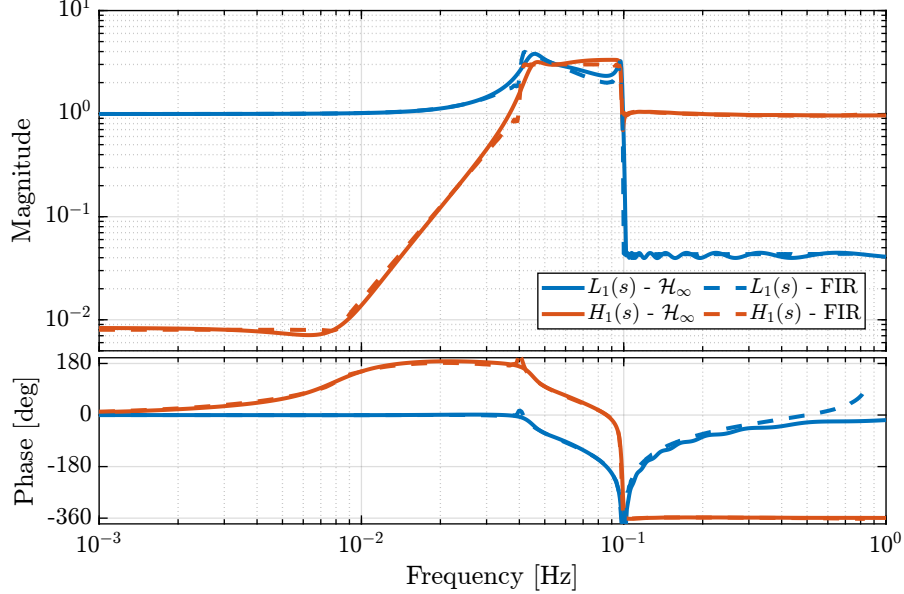

Figure 14: Comparison of the FIR filters (dashed) designed in [5] with the filters obtained with $\mathcal{H}_\infty$ synthesis (solid).

5. Discussion

5.1. "Closed-Loop" complementary filters

An alternative way to implement complementary filters is by using a fundamental property of the classical feedback architecture shown in Fig. 15. This is for instance presented in [7, 13, 33].
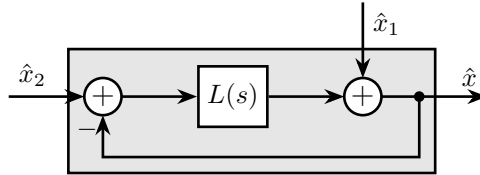

Figure 15: "Closed-Loop" complementary filters.

Consider the feedback architecture of Fig. 15, with two inputs $\hat{x}_1$ and $\hat{x}_2$, and one output $\hat{x}$. The output $\hat{x}$ is linked to the inputs by (18).

$$\hat{x} = \underbrace{\frac{1}{1+L(s)}}_{S(s)} \hat{x}_1 + \underbrace{\frac{L(s)}{1+L(s)}}_{T(s)} \hat{x}_2 \tag{18}$$

As for any classical feedback architecture, we have that the sum of the sensitivity and complementary sensitivity transfer function is equal to one (19).

$$T(s) + S(s) = 1 \tag{19}$$

Therefore, provided that the closed-loop system is stable, the closed-loop system in Fig. 15 is corresponding to two complementary filters. Two sensors can then be merged as shown in Fig. 16.
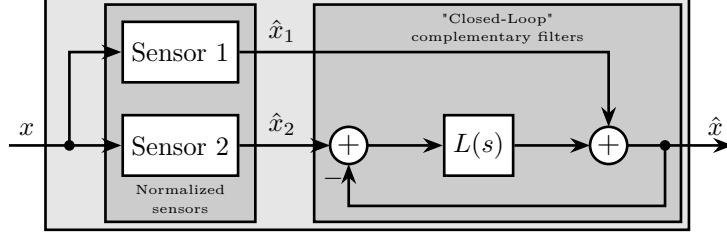

Figure 16: Classical feedback architecture used for sensor fusion.

One of the main advantage of implementing and designing complementary filters using the feedback architecture of Fig. 15 is that all the tools of the linear control theory can be applied for the design of the filters. If one want to shape both $\frac{\hat{x}}{\hat{x}_1}(s) = S(s)$ and $\frac{\hat{x}}{\hat{x}_2}(s) = T(s)$, the $\mathcal{H}_\infty$ mixed-sensitivity synthesis can be easily applied.

To do so, weighting functions $W_1(s)$ and $W_2(s)$ are added to respectively shape $S(s)$ and $T(s)$ (Fig. 17a). Then the system is re-organized to form the generalized plant $P_L(s)$ shown in Fig. 17b. The $\mathcal{H}_\infty$ mixed-sensitivity synthesis can finally be performed by applying the $\mathcal{H}_\infty$ synthesis to the generalized plant $P_L(s)$ which is described by (20).

$$\begin{bmatrix} z \\ v \end{bmatrix} = P_L(s) \begin{bmatrix} w_1 \\ w_2 \\ u \end{bmatrix}; \quad P_L(s) = \begin{bmatrix} W_1(s) & 0 & 1 \\ -W_1(s) & W_2(s) & -1 \end{bmatrix} \tag{20}$$

The output of the synthesis is a filter $L(s)$ such that the "closed-loop" $\mathcal{H}_\infty$ norm from $[w_1, \ w_2]$ to z is less than one (21).

$$\left\| \begin{matrix} \frac{z}{w_1} \\ \frac{z}{w_2} \end{matrix} \right\|_\infty = \left\| \begin{matrix} \frac{1}{1+L(s)} W_1(s) \\ \frac{L(s)}{1+L(s)} W_2(s) \end{matrix} \right\|_\infty \leq 1 \tag{21}$$

If the synthesis is successful, two complementary filters are obtained with their magnitudes bounded by the inverse magnitudes of the weighting functions. The sensor fusion can then be implemented as shown in Fig. 16 using the feedback architecture or more classically as shown in Fig. 1 by defining the two complementary filters as in (22).

$$H_1(s) = \frac{1}{1 + L(s)}; \quad H_2(s) = \frac{L(s)}{1 + L(s)} \tag{22}$$

The two architectures are equivalent regarding their inputs/outputs relationships.

As an example, two "closed-loop" complementary filters are designed using the $\mathcal{H}_\infty$ mixed-sensitivity synthesis. The weighting functions are designed using formula (14) with parameters shown in Table 1. After synthesis, a filter $L(s)$ is obtained, its magnitude is shown in Fig. 18 by the dashed line. The "closed-loop" complementary filters are compared with the inverse magnitude of the weighting functions in Fig. 18 confirming that the synthesis is successful. The obtained "closed-loop" complementary filters are indeed equal to the ones obtained in Section 3.4.
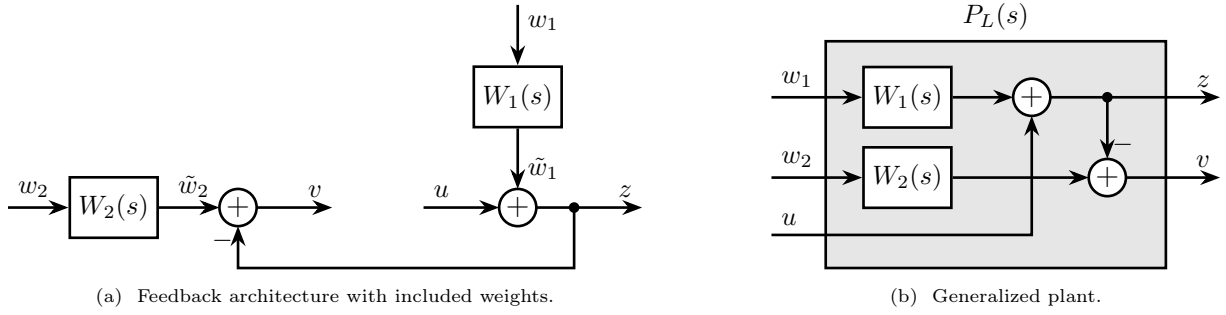
(a) Feedback architecture with included weights.

(b) Generalized plant.

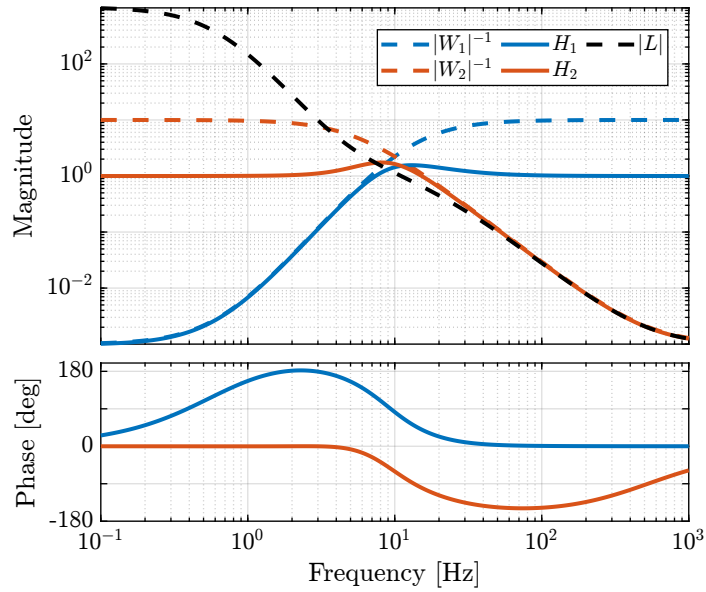Figure 17: $\mathcal{H}_\infty$ mixed-sensitivity synthesis.

Figure 18: Bode plot of the obtained complementary filters after $\mathcal{H}_\infty$ mixed-sensitivity synthesis.

5.2. Synthesis of more than two Complementary Filters

Some applications may require to merge more than two sensors [23, 26]. For instance at the LIGO [27], three sensors (an LVDT, a seismometer and a geophone) are merged to form a super sensor (Fig. 11).

When merging $n > 2$ sensors using complementary filters, two architectures can be used as shown in Fig. 19. The fusion can either be done in a "sequential" way where $n-1$ sets of two complementary filters are used (Fig. 19a), or in a "parallel" way where one set of n complementary filters is used (Fig. 19b).

In the first case, typical sensor fusion synthesis techniques can be used. However, when a parallel architecture is used, a new synthesis method for a set of more than two complementary filters is required as only simple analytical formulas have been proposed in the literature {[23, 26]}. A generalization of the proposed synthesis method of complementary filters is presented in this section.
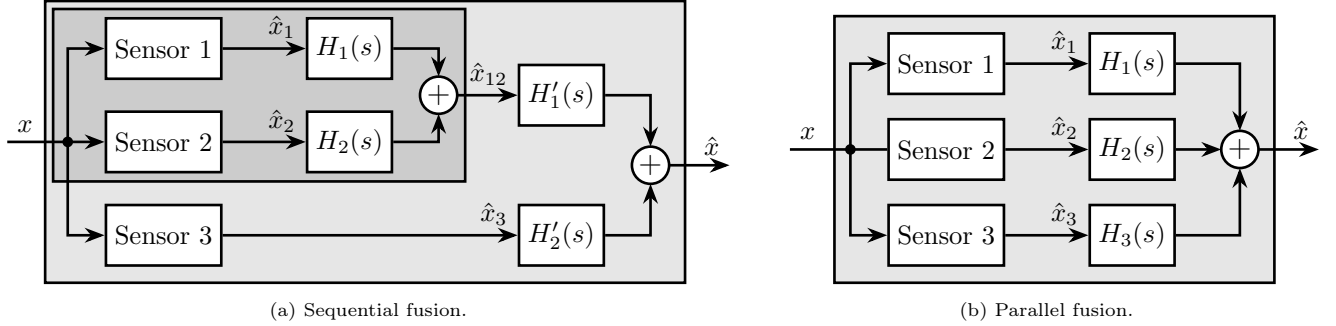

(a) Sequential fusion.

(b) Parallel fusion.

Figure 19: Possible sensor fusion architecture when more than two sensors are to be merged.

The synthesis objective is to compute a set of n stable transfer functions $[H_1(s), H_2(s), \ldots, H_n(s)]$ such that conditions (23a) and (23b) are satisfied.

$$\sum_{i=0}^{n} H_i(s) = 1 \tag{23a}$$

$$|H_i(j\omega)| < \frac{1}{|W_i(j\omega)|}, \quad \forall \omega, \; i = 1 \ldots n \tag{23b}$$

where $[W_1(s), W_2(s), \ldots, W_n(s)]$ are weighting transfer functions that are chosen to specify the maximum wanted norms of the complementary filters during the synthesis.

Such synthesis objective is closely related to the one described in Section 3.1, and indeed the proposed synthesis method is a generalization of the one presented in Section 3.2.

Before presenting the generalized synthesis method, the case with three sensors is presented. Consider the generalized plant $P_3(s)$ shown in Fig. 20a which is also described by (24).

$$\begin{bmatrix} z_1 \\ z_2 \\ z_3 \\ v \end{bmatrix} = P_3(s) \begin{bmatrix} w \\ u_1 \\ u_2 \end{bmatrix}; \quad P_3(s) = \begin{bmatrix} W_1(s) & -W_1(s) & -W_1(s) \\ 0 & W_2(s) & 0 \\ 0 & 0 & W_3(s) \\ 1 & 0 & 0 \end{bmatrix} \tag{24}$$

Applying the $\mathcal{H}_\infty$ synthesis on the generalized plant $P_3(s)$ is equivalent as to find two stable filters $[H_2(s), H_3(s)]$ (shown in Fig. 20b) such that the $\mathcal{H}_\infty$ norm of the transfer function from w to $[z_1, z_2, z_3]$ is less than one (25).

$$\left\| \begin{matrix} [1 - H_2(s) - H_3(s)] \, W_1(s) \\ H_2(s)W_2(s) \\ H_3(s)W_3(s) \end{matrix} \right\|_\infty \leq 1 \tag{25}$$

15

(a) Generalized plant.
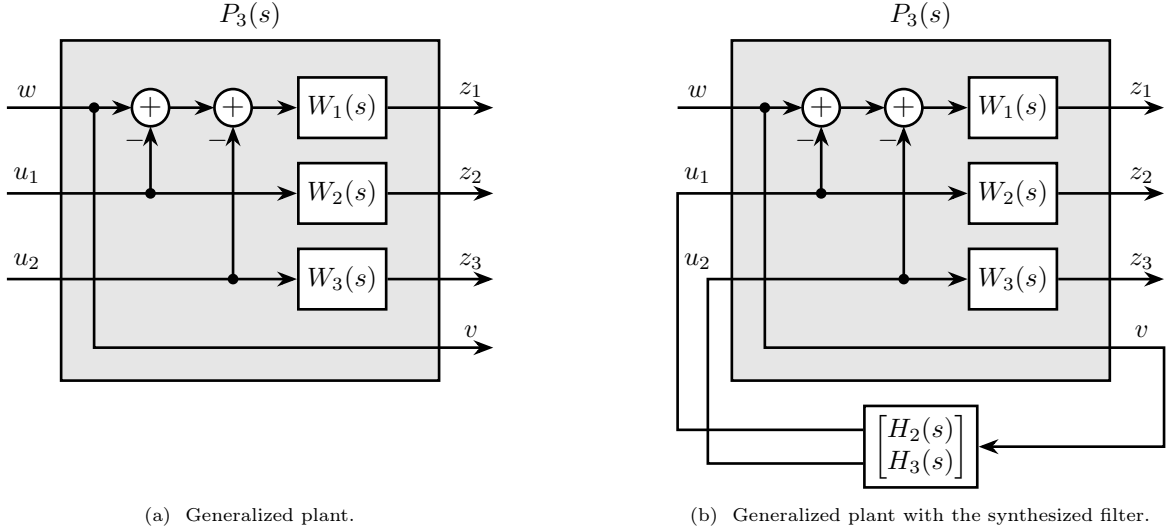
(b) Generalized plant with the synthesized filter.

Figure 20: Architecture for the $\mathcal{H}_\infty$ synthesis of three complementary filters.

By defining $H_1(s) \triangleq 1 - H_2(s) - H_3(s)$, the proposed $\mathcal{H}_\infty$ synthesis solves the design problem (23) with $n = 3$.

An example is given to validate the method where three sensors are used in different frequency bands. For instance a displacement sensor from DC up to 1 Hz, a geophone from 1 to 10 Hz and an accelerometer above 10 Hz. Three weighting functions are designed using formula (14) and their inverse magnitudes are shown in Fig. 21 (dashed curves). The $\mathcal{H}_\infty$ synthesis is performed on the generalized plant $P_3(s)$ and the bode plot of the obtained complementary filters are shown in Fig. 21 (solid lines).
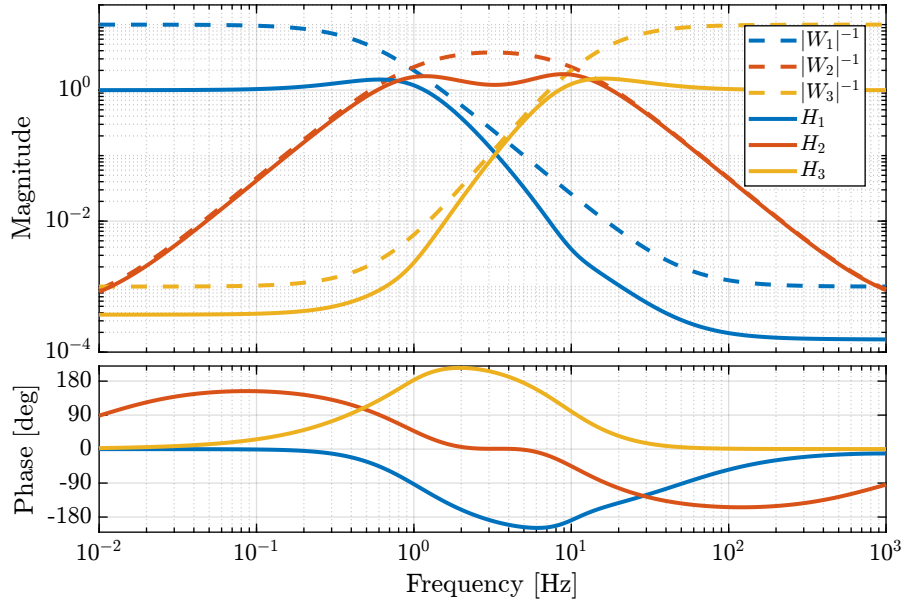

Figure 21: Bode plot of the inverse weighting functions and of the three complementary filters obtained using the $\mathcal{H}_\infty$ synthesis.

Even though there might not be any practical application for a set of more than 3 complementary filters, it can still be designed using the same procedure. A set of n complementary filters can be shaped using the generalized plant $P_n(s)$ described by (26).

16

$$\begin{bmatrix} z_1 \\ \vdots \\ z_n \\ v \end{bmatrix} = P_n(s) \begin{bmatrix} w \\ u_1 \\ \vdots \\ u_{n-1} \end{bmatrix}; \quad P_n(s) = \begin{bmatrix} W_1 & -W_1 & \dots & \dots & -W_1 \\ 0 & W_2 & 0 & \dots & 0 \\ \vdots & \ddots & \ddots & \ddots & \vdots \\ \vdots & & \ddots & \ddots & 0 \\ 0 & \dots & \dots & 0 & W_n \\ 1 & 0 & \dots & \dots & 0 \end{bmatrix} \quad (26)$$

6. Conclusion

The sensor fusion robustness and the obtained super sensor noise can be linked to the magnitude of the complementary filters. In this paper, a synthesis method that enables the shaping of the complementary filters norms has been proposed. Several examples were used to emphasize the simplicity and the effectiveness of the proposed method. Links with "closed-loop" complementary filters were highlighted, and the proposed method was generalized for designing a set of more than two complementary filters.

The future work will aim at developing a complementary filter synthesis method that minimizes the super sensor noise while ensuring the robustness of the fusion.

Data Availability

Matlab [29] was used for this study. The source code is available under a MIT License and archived in Zenodo [34].

References

[1] J. Bendat, Optimum filters for independent measurements of two related perturbed messages, IRE Transactions on Circuit Theory (1957). doi:10.1109/tct.1957.1086345.

[2] F. Shaw, K. Srinivasan, Bandwidth enhancement of position measurements using measured acceleration, Mechanical Systems and Signal Processing 4 (1) (1990) 23–38. doi:10.1016/0888-3270(90)90038-M.

[3] M. Zimmermann, W. Sulzer, High bandwidth orientation measurement and control based on complementary filtering, Robot Control (1992). doi:10.1016/B978-0-08-041276-4.50093-5.

[4] H. G. Min, E. T. Jeung, Complementary filter design for angle estimation using mems accelerometer and gyroscope, Department of Control and Instrumentation, Changwon National University, Changwon, Korea (2015) 641–773.

[5] W. Hua, Low frequency vibration isolation and alignment system for advanced LIGO, Ph.D. thesis, stanford university (2005). doi:10.1117/12.552518.

[6] W. Hua, B. Debra, T. Hardham, T. Lantz, A. Giaime, Polyphase FIR complementary filters for control systems, in: Proceedings of ASPE Spring Topical Meeting on Control of Precision Systems, 2004, pp. 109–114.

[7] A. Plummer, Optimal complementary filters and their application in motion measurement, Proceedings of the Institution of Mechanical Engineers, Part I: Journal of Systems and Control Engineering 220 (6) (2006) 489–507. doi:10.1243/09596518JSCE229.

[8] P. Y. C. H. Robert Grover Brown, Introduction to Random Signals and Applied Kalman Filtering with Matlab Exercises, 4th Edition, Wiley, 2012, isbn:978-0-470-60969-9.

[9] C. Collette, F. Matichard, Sensor fusion methods for high performance active vibration isolation systems, Journal of Sound and Vibration 342 (2015) 1–21. doi:10.1016/j.jsv.2015.01.006.

[10] Y. K. Yong, A. J. Fleming, High-speed vertical positioning stage with integrated dual-sensor arrangement, Sensors and Actuators A: Physical 248 (2016) 184 – 192. doi:10.1016/j.sna.2016.06.042.

[11] A.-J. Baerveldt, R. Klang, A low-cost and low-weight attitude estimation system for an autonomous helicopter, in: Proceedings of IEEE International Conference on Intelligent Engineering Systems, 1997. doi:10.1109/ines.1997.632450.

[12] P. Corke, An inertial and visual sensing system for a small autonomous helicopter, Journal of Robotic Systems 21 (2) (2004) 43–51. doi:10.1002/rob.10127.

[13] A. Jensen, C. Coopmans, Y. Chen, Basics and guidelines of complementary filters for small uas navigation, in: 2013 International Conference on Unmanned Aircraft Systems (ICUAS), 2013. doi:10.1109/ICUAS.2013.6564726.

[14] A. Pascoal, I. Kaminer, P. Oliveira, Navigation system design using time-varying complementary filters, in: Guidance, Navigation, and Control Conference and Exhibit, 1999. doi:10.1109/7.892661.

[15] P. Batista, C. Silvestre, P. Oliveira, Optimal position and velocity navigation filters for autonomous vehicles, Automatica 46 (4) (2010) 767–774. doi:10.1016/j.automatica.2010.02.004.

[16] D. Tjepkema, J. van Dijk, H. Soemers, Sensor fusion for active vibration isolation in precision equipment, Journal of Sound and Vibration 331 (4) (2012) 735–749. doi:10.1016/j.jsv.2011.09.022.

[17] J. van Heijningen, Low-frequency performance improvement of seismic attenuation systems and vibration sensors for next generation gravitational wave detectors, Ph.D. thesis, Vrije Universiteit (2018).

[18] T. Lucia, Low frequency optimization and performance of advanced virgo seismic isolation system, Ph.D. thesis, University of Siena (2018).

[19] W. Anderson, E. Fritze, Instrument approach system steering computer, Proceedings of the IRE 41 (2) (1953) 219–228. doi:10.1109/JRPROC.1953.274209.

[20] R. G. Brown, Integrated navigation systems and kalman filtering: a perspective, Navigation 19 (4) (1972) 355–362. doi:10.1002/j.2161-4296.1972.tb01706.x.

[21] Á. Odry, R. Fuller, I. J. Rudas, P. Odry, Kalman filter for mobile-robot attitude estimation: Novel optimized and adaptive solutions, Mechanical systems and signal processing 110 (2018) 569–589. doi:10.1016/j.ymssp.2018.03.053.

[22] W. T. Higgins, A comparison of complementary and kalman filtering, IEEE Transactions on Aerospace and Electronic Systems (3) (1975) 321–325. doi:10.1109/TAES.1975.308081.

[23] T. Becker, J. A. Fabro, A. S. d. Oliveira, L. P. Reis, Complementary filter design with three frequency bands: Robot attitude estimation, in: International Conference on Autonomous Robot Systems and Competitions, 2015, isbn:978-1-4673-6991-6. doi:10.1109/ICARSC.2015.34.

[24] S. I. Moore, A. J. Fleming, Y. K. Yong, Capacitive instrumentation and sensor fusion for high-bandwidth nanopositioning, IEEE Sensors Letters 3 (8) (2019) 1–3. doi:10.1109/lsens.2019.2933065.

[25] T.-J. Yeh, C.-Y. Su, W.-J. Wang, Modelling and control of a hydraulically actuated two-degree-of-freedom inertial platform, Proceedings of the Institution of Mechanical Engineers, Part I: Journal of Systems and Control Engineering 219 (6) (2005) 405–417. doi:10.1243/095965105x33527.

[26] D. Stoten, Fusion of kinetic data using composite filters, Proceedings of the Institution of Mechanical Engineers, Part I: Journal of Systems and Control Engineering 215 (5) (2001) 483–497. doi:10.1177/095965180121500505.

[27] F. Matichard, B. Lantz, R. Mittleman, K. Mason, J. Kissel, et al., Seismic isolation of advanced LIGO: Review of strategy, instrumentation and performance, Classical and Quantum Gravity 32 (18) (2015) 185003. `doi:10.1088/0264-9381/32/18/185003`.

[28] T. Dehaeze, M. Vermat, C. Collette, Complementary filters shaping using $\mathcal{H}_\infty$ synthesis, in: 7th International Conference on Control, Mechatronics and Automation (ICCMA), 2019, pp. 459–464. `doi:10.1109/ICCMA46720.2019.8988642`.

[29] MATLAB, version 9.9.0 (R2020b), The MathWorks Inc., Natick, Massachusetts, 2020.

[30] T. Sekiguchi, A study of low frequency vibration isolation system for large scale gravitational wave detectors, Ph.D. thesis, University of Tokyo (2016).

[31] W. Hua, R. Adhikari, D. B. DeBra, J. A. Giaime, G. D. Hammond, C. Hardham, M. Hennessy, J. P. How, B. T. Lantz, M. Macinnis, et al., Low-frequency active vibration isolation for advanced LIGO, in: Gravitational Wave and Particle Astrophysics Detectors, Vol. 5500, International Society for Optics and Photonics, 2004, pp. 194–205.

[32] J. F. Sturm, Using SeDuMi 1.02, a matlab toolbox for optimization over symmetric cones, Optimization methods and software 11 (1-4) (1999) 625–653. `doi:10.1080/10556789908805766`.

[33] R. Mahony, T. Hamel, J.-M. Pflimlin, Complementary filter design on the special orthogonal group so(3), in: Proceedings of the 44th IEEE Conference on Decision and Control, 2005. `doi:10.1109/cdc.2005.1582367`.

[34] T. Dehaeze, A New Method of Designing Complementary Filters for Sensor Fusion Using the $\mathcal{H}_\infty$ Synthesis, Source code on Zenodo (Sep. 2021). `doi:10.5281/zenodo.5361943`.